Satellite-based PM$_{2.5}$ estimation using fine-mode aerosol optical thickness over China

Xing Yan [a, b], Wenzhong Shi [b, *], Zhanqing Li [a, c, **], Zhengqiang Li [d], Nana Luo [e], Wenji Zhao [f], Haofei Wang [d], Xue Yu [f]

[a] State Key Laboratory of Earth Surface Processes and Resource Ecology, College of Global Change and Earth System Science, Beijing Normal University, Beijing, China
[b] Department of Land Surveying and Geo-Informatics, The Hong Kong Polytechnic University, Hong Kong
[c] Department of Atmospheric and Oceanic Science, and Earth System Science Interdisciplinary Center, University of Maryland, College Park, MD, USA
[d] State Environmental Protection Key Laboratory of Satellite Remote Sensing, Institute of Remote Sensing and Digital Earth, Chinese Academy of Sciences, Beijing 100101, China
[e] Department of Geography, San Diego State University, 5500 Campanile Dr., San Diego, CA 92182-4493, USA
[f] College of Resource Environment and Tourism, Capital Normal University, Beijing, China

HIGHLIGHTS

- PM$_{2.5}$ was more closely correlated with fine mode AOT than with total AOT.
- A new fine mode fraction was incorporated into the model to retrieve surface PM$_{2.5}$.
- Using a rough estimate of particle density for PM$_{2.5}$ retrieval enhanced the accuracy.
- The method was tested and validated with 30 long-term ground-based observations.

GRAPHICAL ABSTRACT
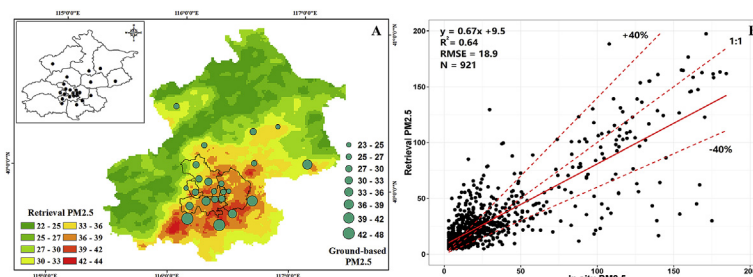
ARTICLE INFO

ABSTRACT

Accurate estimation of ground-level PM$_{2.5}$ from satellite-derived aerosol optical thickness (AOT) presents various difficulties. This is because the association between AOT and surface PM$_{2.5}$ can be affected by many factors, such as the contribution of fine mode AOT (FM-AOT) and the weather conditions. In this study, we compared the total AOT and FM-AOT for surface PM$_{2.5}$ estimation using ground-based measurements collected in Xingtai, China from May to June 2016. The correlation between PM$_{2.5}$ and FM-AOT was higher ($r = 0.74$) than that between PM$_{2.5}$ and total AOT ($r = 0.49$). Based on FM-AOT, we developed a ground-level PM$_{2.5}$ retrieval method that incorporated a Simplified Aerosol Retrieval Algorithm (SARA) AOT, look-up table–spectral deconvolution algorithm (LUT-SDA) fine mode fraction (FMF), and the PM$_{2.5}$ remote sensing method. Due to the strong diurnal variations displayed by the particle density of PM$_{2.5}$, we proposed a pseudo-density for PM$_{2.5}$ retrieval based on real-time visibility data. We applied the proposed method to determine retrieval surface PM$_{2.5}$ concentrations over Beijing from December 2013 to June 2015 on cloud-free days. Compared with Aerosol Robotic Network (AERONET) data, the LUT-SDA FMF was more easily available than the Moderate Resolution Imaging Spectroradiometer (MODIS) FMF. The derived PM$_{2.5}$ results were compared with the ground-based monitoring values (30 stations),

---

* Corresponding author. Dept. of Land Surveying and Geo-Informatics, The Hong Kong Polytechnic University, Hong Kong.
** Corresponding author. ESPRE/GCESS, Beijing Normal University, 19 Xinjiekouwai Street, Haidian District, Beijing 100875, China.
E-mail addresses: lswzshi@polyu.edu.hk (W. Shi), zli@atmos.umd.edu (Z. Li).

yielding an R^2 of 0.64 and root mean square error (RMSE) = 18.9 μg/m^3 (N = 921). This validation demonstrated that the developed method performed well and produced reliable results.

1. Introduction

Particulate matter with an aerodynamic diameter less than 2.5 μm (PM$_{2.5}$) has adverse effects on human health (Anderson et al., 2012). Numerous studies have demonstrated that PM$_{2.5}$ is associated with mortality, respiratory system problems, and lung cancer (Pope et al., 2002; Brook et al., 2010; Kloog et al., 2013). More specifically, a decrease of 10 μg/m^3 in the concentration of PM$_{2.5}$ was associated with an estimated increase in life expectancy of approximately 6 months (Pope et al., 2009). Thus, it is important to accurately assess the distribution of PM$_{2.5}$ concentrations and exposures to guide control measures for mitigating health impacts (Bell et al., 2011; Luo et al., 2014).

Monitoring site measurements of ground-level PM$_{2.5}$ concentrations offer a convenient but rudimentary option for pollution and health studies; their spatial coverage is sparse and limited (Han et al., 2015). Satellite remote sensing has been used in many studies to obtain large-scale PM$_{2.5}$ distributions (Liu et al., 2009; Lee et al., 2011; Chudnovsky et al., 2014; Kloog et al., 2015). The common satellite product for estimating ground-level PM$_{2.5}$ concentration is aerosol optical thickness (AOT). Researchers have determined the relationships between AOT and PM$_{2.5}$ concentration through various approaches, including empirical statistical models (Engel-Cox et al., 2004; Gupta et al., 2006; Schaap et al., 2009; Guo et al., 2014), chemical transport models (Wang et al., 2010; van Donkelaar et al., 2010; Liu et al., 2011; Xu et al., 2013), and physical models (Kokhanovsky et al., 2009).

Most of the recent studies using satellite AOT to derive PM$_{2.5}$ have focused on the total AOT for estimation of ground-level PM$_{2.5}$ (Eeftens et al., 2012; Lee et al., 2012; Luo et al., 2014). However, some researchers reported that fine mode AOT (FM-AOT) has a higher correlation with ground-level PM$_{2.5}$ (Nicolantonio et al., 2007; Zhang and Li, 2013). van Donkelaar et al. (2011) successfully applied FM-AOT for PM$_{2.5}$ estimation in Moscow with high accuracy. Compared with using total AOT to estimate PM$_{2.5}$, Nicolantonio et al. (2007) reported a significant improvement in using FM-AOT; correlation coefficients increased from 0.59 to 0.74 for measurements collected over north Italy in June. Zhang and Li (2013) reported that the relationship between FM-AOT and PM$_{2.5}$ was significantly closer than that between total AOT and PM$_{2.5}$ under hazy weather conditions. Although the correlations with PM$_{2.5}$ are improved by using FM-AOT, there have been few studies comparing total AOT and FM-AOT for estimating PM$_{2.5}$. However, because FM-AOT is used in PM$_{2.5}$ retrieval models, the fine mode fraction (FMF), which is used to separate contributions from smaller and larger particles in AOT, is becoming an increasingly important parameter. Zhang and Li (2015) proposed an expression between Aerosol Robotic Network (AERONET) FMF and volume-to-extinction ratio of fine particulates (VE$_f$) for PM$_{2.5}$ retrieval, and applied the expression using Moderate Resolution Imaging Spectroradiometer (MODIS) FMF. However, AERONET FMF has a very different calculation method than MODIS FMF (Gasso and O'Neill, 2006). Levy et al. (2007) reported that MODIS FMF had a poor correlation with AERONET FMF, and this was also reported by Zhang and Li (2015). Therefore, MODIS FMF may not be suitable for models based on AERONET FMF.

Despite promising recent progress in surface PM$_{2.5}$ estimation

from satellite AOT, uncertainties still exist due to several factors. Toth et al. (2014) found that both the quality of satellite-based AOT retrieval as well as the surface-to-column representativeness of aerosol particles affects the estimation of PM$_{2.5}$ concentration. In addition, the planetary boundary layer height (PBLH) was reported to have a significant impact on the AOT-PM$_{2.5}$ relationship (Gupta and Christopher, 2009); this is because greater PBLH is more favorable for dilution and diffusion of pollutants, which produces low concentrations of surface PM$_{2.5}$ despite high AOT (Qu et al., 2016). Relative humidity (RH) was found to be another key factor that could result in discrepancies between AOT and surface PM$_{2.5}$ (Wang, 2003; Paciorek et al., 2008). Wang et al. (2010) reported a significant improvement in surface PM$_{2.5}$ estimation when a RH correction was incorporated (R^2 increased from 0.35 to 0.66). Furthermore, recent studies have used the MODIS AOT products (MOD04) for PM$_{2.5}$ monitoring, but its spatial resolution is 10 km, which is unsuitable for exposure estimates in urban areas (Jerrett et al., 2005; Luo et al., 2015). Chudnovsky et al. (2013) reported that the spatial resolution of AOT also affected PM$_{2.5}$ accuracy: the correlation between AOT and PM$_{2.5}$ decreased significantly because the AOT resolution was degraded. Although MODIS recently released a 3-km AOT product, the accuracy was less reliable than that of 10-km AOTs (Munchak et al., 2013; Yan et al., 2016).

Yan et al. (2017) proposed a look-up table–spectral deconvolution algorithm (LUT-SDA) method for satellite FMF that showed a high correlation with AERONET FMF. In addition, Bilal et al. (2013) developed a Simplified Aerosol Retrieval Algorithm (SARA) to derive AOT from MODIS, which provided up to 500-m spatial resolution AOT and has been validated in Hong Kong and Beijing (Bilal et al., 2014). Thus, in this study, we used field data to compare the total AOT and FM-AOT with the surface particulate matter concentration. Then, we developed a ground-level PM$_{2.5}$ retrieval model for satellite data based on FM-AOT, which incorporated the LUT-SDA (Yan et al., 2017), SARA (Bilal et al., 2013), and the PM$_{2.5}$ remote sensing method (Zhang and Li, 2015).

2. Data and methods

2.1. Ground-based experiment at Xingtai

To compare the correlations between total AOT and FM-AOT with surface PM$_{2.5}$, we performed a ground-based experiment in Xingtai city, Hebei province, China, (37.18°N, 114.36°E, Fig. 1). Xingtai is an important transportation hub and center of heavy industry (Chen et al., 2017). It also has high raw coal consumption of more than 3000 kt (Cheng et al., 2017). The key industries in Xingtai are construction, coal, and the metallurgy, all of which produce high emissions of air pollutants (Wang et al., 2015b).

The surface particulate matter concentration was obtained using a GrayWolf 6-channel handheld particle/mass meter (PC-3016A). As a stand-alone meter, the GrayWolf PC-3016A can measure particle concentration (μg/m^3) with a size range of 0.3–10.0 μm (https://www.wolfsense.com/). Thus, besides PM$_{2.5}$, we also collected PM$_1$ concentration data in this study. Here the PM data is to compare the relationship between total AOT, FM-AOT and PM$_{2.5}$ at Xingtai.

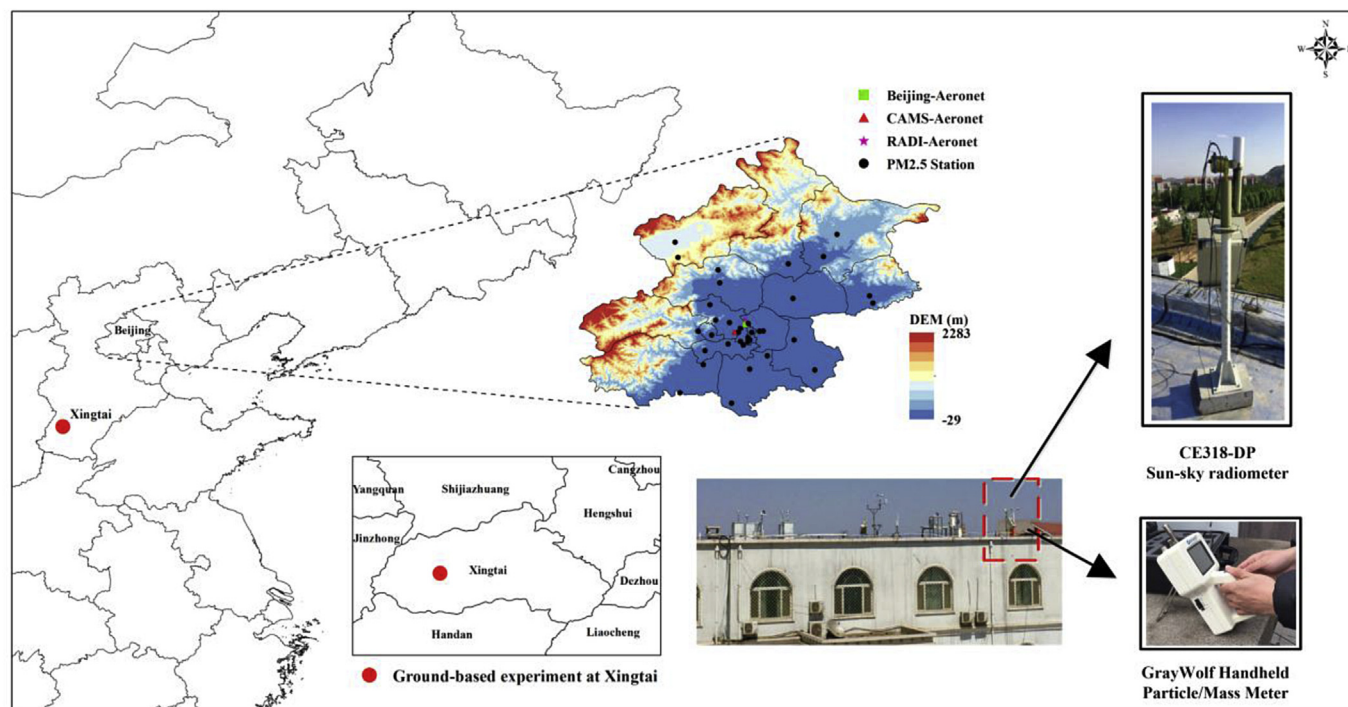The columnar aerosol data were measured using a CE318-DP

Fig. 1. Ground-based experiment in Xingtai and satellite validation in Beijing.

sun-sky radiometer (AOT uncertainties are 0.01–0.02, Li et al. (2016)). This polarized version CE318 belongs to the Sun-sky radiometer Observation NETwork (SONET) and the collected data had been uploaded to AERONET SONET_Xingtai (Li et al., 2016). The aerosol data used in this research is corresponding to the level 1.5 of the AERONET (Holben et al., 1998).

Meteorological parameters including temperature (T, uncertainties are 0.2 °C), RH (uncertainties are 1%–5%), wind speed (WS, uncertainties are 0.5 m/s −1 m/s), wind direction (WD, uncertainties are 5°–10°) and visibility (VIS, uncertainties are 20%) were simultaneously recorded by an automatic meteorological station at the same location as the study area (WMO, 2008). All measurements in Xingtai were collected from 1 May to 1 Jun 2016.

2.2. Satellite AOT

The MODIS MOD02HKM, MOD03, and MOD09 cloud-free data were acquired (https://ladsweb.nascom.nasa.gov) for AOT retrieval, as shown in Table 1. In addition, Collection 6 MODIS aerosol products (C6 MOD04) were obtained for this study, and the C6 cloud mask data (Aerosol_Cldmsk_Land_Ocean) were extracted from MOD04 and used for cloud screening in aerosol retrieval algorithm. The SARA was applied in the Beijing area due to its high accuracy. AOT derived by SARA was validated in Beijing and the results showed a close correlation with AERONET AOT (0.97–0.99), with a small root mean square error (RMSE) 0.067–0.133 (Bilal et al., 2014). In this study, 550 nm AOT was retrieved by SARA and its comparison with AERONET was showed in Supplementary Fig. S1. It shows the majority of the observations (81%) are within the error range $\pm (0.05 + 0.15_{\text{AERONET AOT}})$, which indicates that the retrieved AOT values are of good quality.

2.3. AERONET

The AERONET program is a federation of ground-based remote

Table 1
The MODIS data used in this study.

Day	Month	Year	Day	Month	Year
11	12	2013	13	11	2014
12	12	2013	17	11	2014
14	12	2013	22	11	2014
26	12	2013	1	12	2014
28	12	2013	3	12	2014
30	12	2013	17	12	2014
1	1	2014	24	12	2014
3	1	2014	31	12	2014
22	1	2014	2	1	2015
4	2	2014	11	1	2015
2	5	2014	6	1	2015
7	5	2014	27	1	2015
18	5	2014	30	1	2015
3	6	2014	5	2	2015
12	6	2014	17	2	2015
27	6	2014	26	2	2015
28	6	2014	3	3	2015
10	7	2014	11	3	2015
12	7	2014	24	4	2015
15	8	2014	26	4	2015
25	8	2014	4	5	2015
3	9	2014	7	5	2015
8	9	2014	19	5	2015
9	9	2014	26	5	2015
15	9	2014	2	6	2015
16	10	2014	8	6	2015
17	10	2014	18	6	2015

sensing aerosol networks (Holben et al., 2001). The AERONET collaboration provides globally distributed observations of spectral AOT, inversion products, and other AOT-dependent products. AOT data are computed for three data quality levels: Level 1.0 (unscreened), Level 1.5 (cloud-screened), and Level 2.0 (cloud-screened and quality-assured). In this study, 550 nm AOT (interpolated by 675 nm and 440 nm) and FMF were collected at the AERONET sites in Beijing (Level 2), CAMS (Level 2), and RADI (only

Level 1.5 available) from December 2013 to June 2015 for SARA and validation purposes.

2.4. Beijing $PM_{2.5}$

Hourly ground-measured $PM_{2.5}$ data over the Beijing region from December 2013 to June 2015 were acquired from the Beijing Municipal Environmental Monitoring Center (http://zx.bjmemc. com.cn) for the proposed model validation. The $PM_{2.5}$ monitoring sites, shown in Fig. 1, are mainly located in urban areas, with a few in rural areas. Measurements of $PM_{2.5}$ concentration were based on the Chinese National Ambient Air Quality Standard (GB3095-2012), using the tapered element oscillating microbalance method (TEOM) and the beta-attenuation method (Li et al., 2015).

2.5. LUT-SDA FMF

As described in Yan et al. (2017), the LUT-SDA has been developed for satellite images based on only two wavelengths of AOT to solve the FMF problem. This method is based on the SDA currently used in AERONET. Thus, the outcome of the LUT-SDA is a good match to that of AERONET and is suitable as an input parameter for the AERONET FMF-based model. The LUT-SDA builds a LUT to retrieve the FMF using satellite-derived AOT and Ångström exponent, the detailed algorithm is shown in Supplementary Fig. S2. To build a LUT, a set of hypothetical FMF (η) and Ångström exponent derivative (α') values are imported to the SDA along with the satellite-determined Ångström exponent (α) to derive the Ångström exponent of fine mode aerosols (αf). The LUT-SDA successfully applied to MODIS data not only verified the application to the urban scale (Beijing), but also its expansion to large areas. The retrieved FMF images represent the spatial distribution of the fine aerosol contribution to the total AOT with complex surface types. Therefore, in this study, we used the LUT-SDA for the retrieval FMF for FM-AOT and correlated it with $PM_{2.5}$ estimations.

2.6. PBLH and RH

The Weather Research and Forecasting (WRF) model (ver. 3.6.1) was applied to produce the required PBLH and RH values. The WRF model is a mesoscale numerical weather prediction system that has been validated for producing accurate simulation of meteorological data (Skamarock et al., 2005; Grguric et al., 2014). Initial and boundary conditions were from the National Centers for Environmental Prediction (NCEP) Final (FNL) Operational Global Analysis data (http://rda.ucar.edu/datasets/ds083.2/). NCEP FNL is provided globally at 1° resolution every 6 h. The physics options selected for the WRF simulation for this study were the same as in Zheng et al. (2015), which is also shown in Supplementary Table S1.

2.7. Ground-level $PM_{2.5}$ retrieval model

Zhang and Li (2015) developed a $PM_{2.5}$ remote sensing method for ground-level $PM_{2.5}$ estimation, which they validated in Jinhua city, China (Li et al., 2016). This method proposed a relationship between AOT and $PM_{2.5}$ concentration based on AERONET data, which included FM-AOT conversion, fine particle volume calculation, and PBLH and RH correction. The surface $PM_{2.5}$ concentration can be obtained by the following equation (Zhang and Li, 2015):

$$PM_{2.5} = AOT \cdot \frac{FMF \cdot VE_f \cdot \rho_{f \cdot dry}}{PBLH \cdot f(RH)} \quad (1)$$

where AOT is retrieved from satellite, FMF is fine mode fraction calculated by LUT-SDA, VE_f is the columnar volume-to-extinction

ratio of fine particulates, $\rho_{f \cdot dry}$ is density of dry $PM_{2.5}$, PBLH is the planetary boundary layer height and f (RH) is the optical hydroscopic growth function. VE_f can be calculated by (Zhang and Li, 2015):

$$VE_f = 0.2887FMF^2 - 0.4663FMF + 0.356 \quad (0.1 \leq FMF \leq 1.0) \quad (2)$$

In this study, f (RH) is based on Chen et al. (2015):

$$f(RH) = \begin{cases} 1.02 \times (1 - RH/100)^{-0.21 \times RH/100} & (RH/100 < 0.6) \\ 1.08 \times (1 - RH/100)^{-0.26 \times RH/100} & (RH/100 \geq 0.6) \end{cases} \quad (3)$$

$\rho_{f \cdot dry}$ is assumed to have a constant value of 1.5 g/cm^3 in Zhang and Li (2015) and Li et al. (2016). However, in this study, we assumed that $\rho_{f \cdot dry}$ varies daily (further discussion is in Section 4.2), and then proposed a pseudo-density of $PM_{2.5}$ (ρ_{pseudo}) to substitute for the daily-varied $\rho_{f \cdot dry}$, which can be calculated by ground-based measurements. Thus based on Eq. (1), the pseudo-density of $PM_{2.5}$ is computed as follow:

$$\rho_{pseudo} = \frac{PM_{2.5}^V \cdot PBLH \cdot f(RH)}{AOT \cdot FMF \cdot VE_f} \quad (4)$$

where AOT and FMF are obtained from AERONET stations corresponding to satellite overpass, and PBLH and f (RH) are produced by WRF.

In Eq (4), $PM_{2.5}^V$ is calculated from visibility (VIS) data. Previous studies indicated that $PM_{2.5}$ can be calculated from VIS using the following power function (Leung et al., 2008; Bai et al., 2016):

$$PM_{2.5}^V = A \cdot x^B \quad (5)$$

where x is visibility (VIS) (km), which was obtained from weather station for Beijing (https://www.wunderground.com/). The A and B parameters in this equation are given in Table 2 (Chen et al., 2010). Chen et al. (2010) indicated that it easily causes fog when RH>90%, thus it is not suitable for the estimation of $PM_{2.5}$ from VIS under this weather condition.

A schematic diagram of the ground-level $PM_{2.5}$ retrieval method used in this study is shown in Fig. 2. The method consists of two main steps: (i) calculation of ρ_{pseudo} using VIS data using Eq (4); and (ii) incorporation of ρ_{pseudo} in Eq (1) with SARA-AOT, LUT-SDA FMF, and the PBLH and RH correction for surface $PM_{2.5}$ retrieval. As mentioned in Zhang and Li (2015), the result of Eq. (1) is in mg/m^3, and should be divided by 1000 for comparison with the in situ measurements in μg/m^3.

3. Ground-based experiment in Xingtai

3.1. Dependence of PM on meteorological parameters

Descriptive statistics for the data obtained in Xingtai are presented in Supplementary Table S2. The PM and Meteorological data are recorded each 10 min, and thus there are totally 19 414 data

Table 2
Power function for $PM_{2.5}^V$ (x is VIS in km).

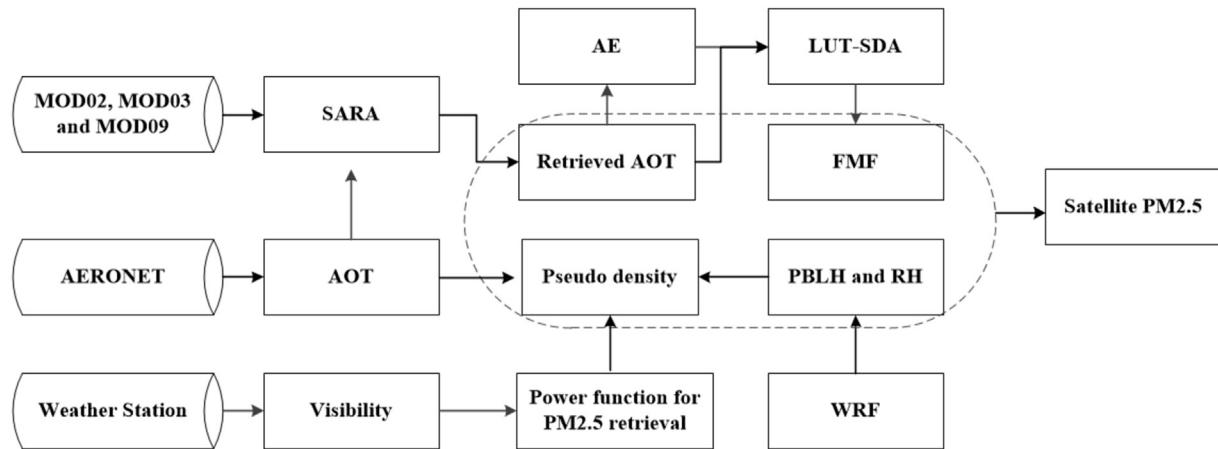| Relative humidity	Power function for $PM_{2.5}^V$ (mg/m^3)
RH < 70%	$PM_{2.5}^V = 0.6977x^{-0.9517}$
70%≤RH≤80%	$PM_{2.5}^V = 0.3628x^{-1.028}$
80% < RH≤90%	$PM_{2.5}^V = 0.2957x^{-0.9463}$

Fig. 2. Schematic diagram of the ground-level PM$_{2.5}$ retrieval model.

obtained; however, VIS N is finally 19 394 since some measurements are missing. Due to the cloud-screened process, the aerosol data are 1 196. Although the mean PM$_1$ and PM$_{2.5}$ were 28.87 µg/m^3, and 45.14 µg/m^3, respectively, indicating a moderate health risk level, their standard deviations were 21.65 µg/m^3, and 32.19 µg/m^3, respectively, which indicates significant variation in the surface PM concentration during the study period. Fig. 3 shows the time series of PM$_1$, PM$_{2.5}$, T, RH, and VIS from 1 May to 1 June 2016 in Xingtai. It can be seen that there was a heavy pollution event from 9 to 12 May 2016 (highlighted in gray). On those days, the PM$_{2.5}$ and PM$_1$ rose as high as 290 µg/m^3, and 135 µg/m^3, respectively, and VIS decreased significantly to 4868 m.

The correlations between PM$_{2.5}$ and meteorological data are shown in Fig. 4. PM$_{2.5}$ was significantly correlated with WS, RH, and VIS. However, T changes did not significantly affect PM$_{2.5}$ concentrations, and we observed a small negative correlation (r = −0.107). Dawson et al. (2007) proposed that PM$_{2.5}$ levels display an almost negligible response to T changes in summer, largely due to increases in sulfate canceling out any decrease in nitrate and organics. RH was highly correlated with PM$_{2.5}$ (r = 0.637), which is in agreement with the findings of Luo et al. (2014). Furthermore, Elminir (2005) reported that an increase in humidity reflects an updraft of boundary layer air masses to 3 km, which may cause higher levels of air pollution. Thus, RH should be taken into account
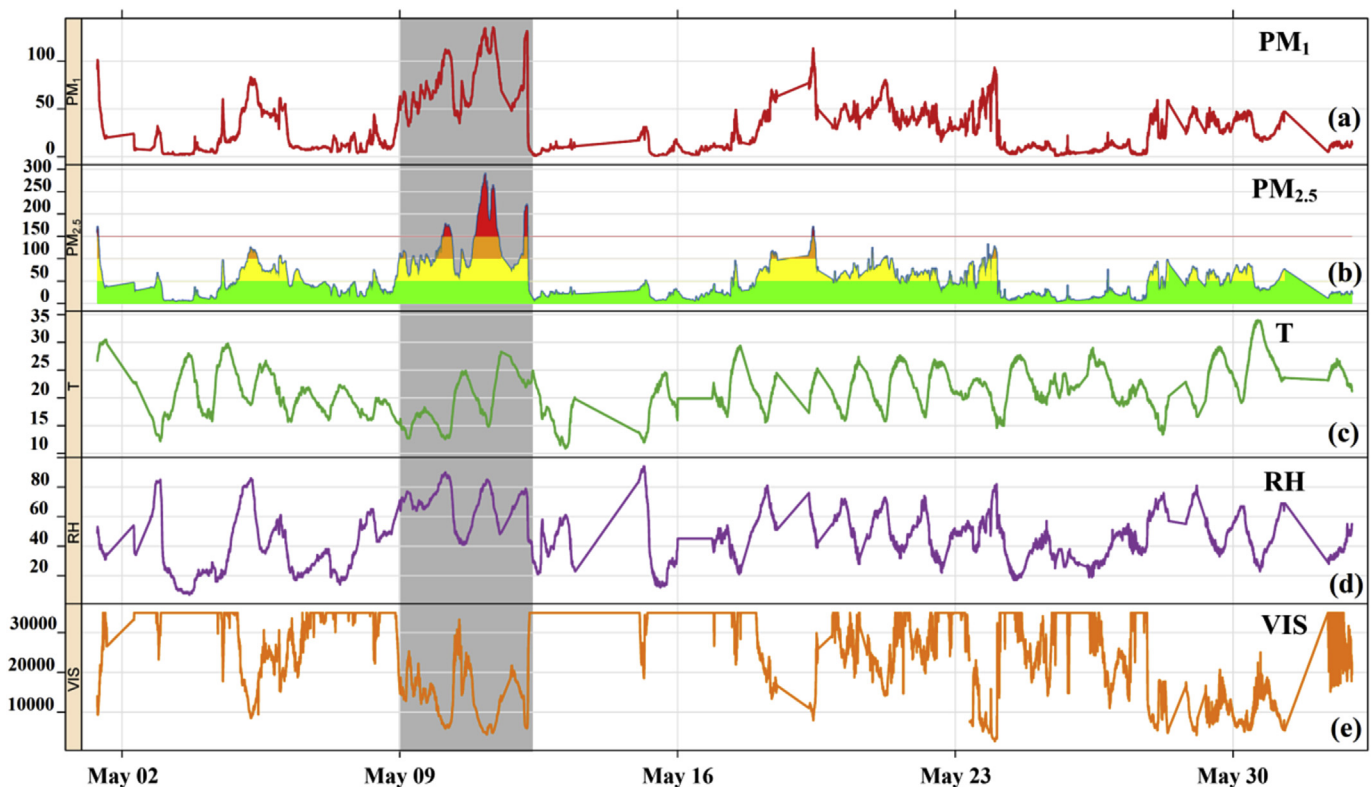

Fig. 3. Time series of (a) PM$_1$, (b) PM$_{2.5}$, (c) temperature (T), (d) relative humidity (RH), and (e) visibility (VIS) in Xingtai, China. The gray highlighted area is the most heavily polluted during the experiment. The shaded colors in (b): the green is 0–50 µg/m^3, the yellow is 50–100 µg/m^3, the orange is 100–150 µg/m^3, and the red is greater than 150 µg/m^3. (For interpretation of the references to colour in this figure legend, the reader is referred to the web version of this article.)
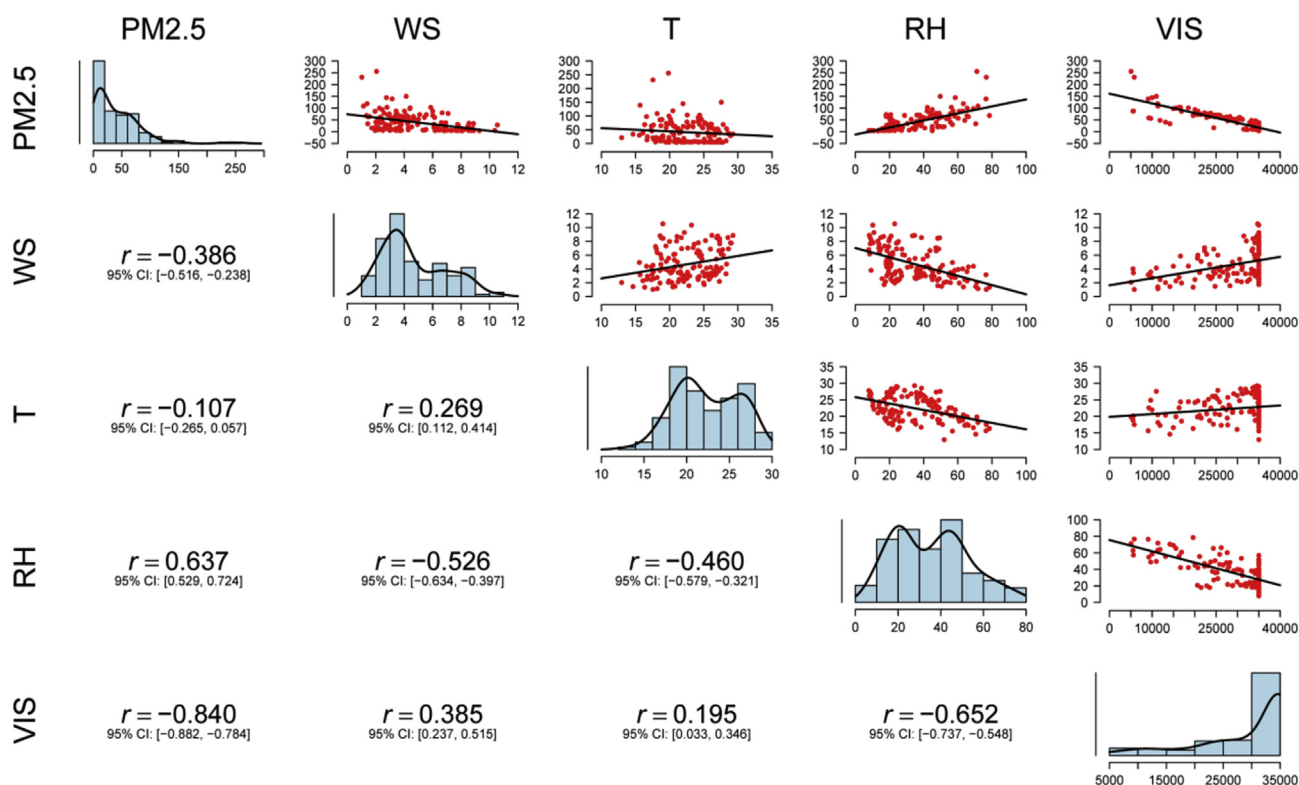
Fig. 4. Correlations between PM$_{2.5}$ and meteorological data. The bar plots are the histogram of observations with a fitted curve, and the scatter plots show the relationships among variables with a fitted line. The r is the correlation coefficient and its 95% confidence interval (CI) is also presented.

as an important factor in surface PM$_{2.5}$ estimation models.

VIS and PM$_{2.5}$ had the most significant anti-correlation (r = −0.840). The main reason for this is that fine particulate matter can scatter and absorb sunlight easily (Liu et al., 2014). Zhao et al. (2011) reported that, based on the negative correlations between VIS and PM$_{2.5}$ concentration, aerosols could cause a greater degree of VIS impairment in the summer months. We also observed a similarly strong negative correlation, which due to the WS being low during the study period, as shown in Supplementary Table S2 (mean = 3.74 m/s, Q3 = 4.70 m/s). Wang et al. (2006) reported that a WS of less than 7.0 m/s produced a high correlation between VIS and PM$_{2.5}$, with the correlation increasing with decreasing WS. Thus, it is appropriate to use VIS to estimate surface PM$_{2.5}$ concentration, as reported by Chen et al. (2010). The use of VIS to improve the retrieval accuracy of PM$_{2.5}$ will be discussed further in Section 4.2.

3.2. Comparison between total AOT and FM-AOT for PM$_{2.5}$ estimation

Fig. 5 shows time series of total AOT, FM-AOT, and FMF. The orange-shaded areas shows when the total AOT was much higher than FM-AOT, which indicates that coarse mode AOT accounted for a major proportion of the total AOT. However, on the days around 8 May 2016, the FM-AOT was very similar to total AOT, and the FMF was approximately 0.93, indicating that FM-AOT accounted for most of the total AOT on those days (indicated by the rectangle with broken red line). The time series of FMF in Fig. 5 also reveals significant variation in the ratio between FM-AOT and total AOT among different days. Kim et al. (2007) observed that the monthly mean FMF varied from 0.60 (December) to 0.77 (July), which reflected a marked difference between FM-AOT and total AOT,

associated with different air pollution conditions.

The comparison between the PM$_{2.5}$ retrieved from total AOT and that from FM-AOT is shown in Fig. 6. In total, 146 hourly data values were collected for statistical correlation analysis. The correlation between total AOT and PM$_{2.5}$ was r = 0.49, with three obvious outliers highlighted by colored circles in Fig. 6. However, the correlation between FM-AOT and PM$_{2.5}$ (r = 0.74) was clearly higher than that between total AOT and PM$_{2.5}$. When the FMF correction was incorporated, the three outliers disappeared and the data were close to the fitted line. The comparison between total AOT and FM-AOT with PM$_1$ is also presented in Fig. 6. It can be seen that FM-AOT was significantly more closely correlated with PM$_1$ than was total AOT with PM$_1$ (r increased from 0.50 to 0.82), and the correlation was higher than with PM$_{2.5}$ (r = 0.74). This is because the range of the upper limits of the radius for FM-AOT in AERONET is 0.439–0.992 μm, which contains all of the fine particles of PM$_1$ (Wang et al., 2015a). Thus, these comparisons indicate that the FM-AOT is more suitable for fine particulate matter estimation, which is in agreement with the research of Nicolantonio et al. (2007), and Zhang and Li (2013).

4. Ground-level PM$_{2.5}$ estimation based on satellite FM-AOT

4.1. LUT-SDA FMF

As shown in Eqs. (1) and (2), FMF is an important parameter that can directly affect not only VE$_f$ but also final PM$_{2.5}$ outcomes. Thus, reliable FMF values are necessary for the PM$_{2.5}$ retrieval model. Although the MODIS aerosol products provide the FMF data, its retrieval accuracy over land is highly uncertain (Levy et al., 2010). Thus, in this study, LUT-SDA was applied to improve FMF. Comparisons of FMF values calculated from the LUT-SDA versus those
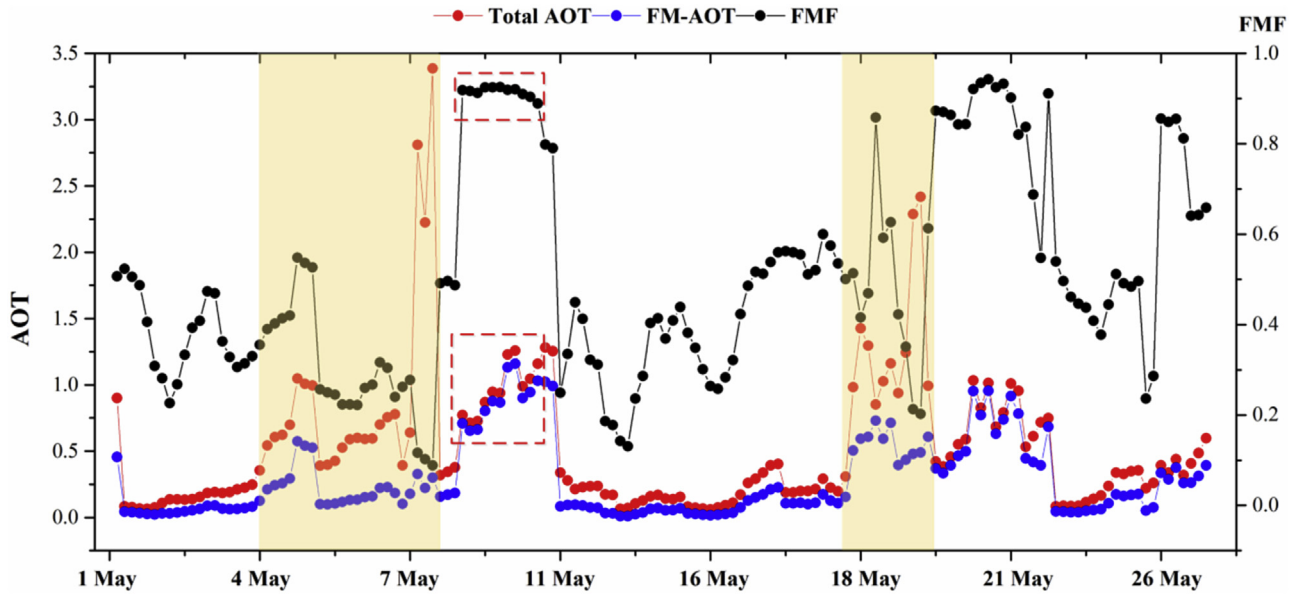
Fig. 5. Time series of total aerosol optical thickness (AOT), fine mode AOT (FM-AOT), and fine mode fraction (FMF) in Xingtai, China. The shaded areas present that the total AOT is much higher than FM-AOT. The red dotted rectangles show that the FM-AOT, especially thoes with high FMF values, is very similar to total AOT. (For interpretation of the references to colour in this figure legend, the reader is referred to the web version of this article.)
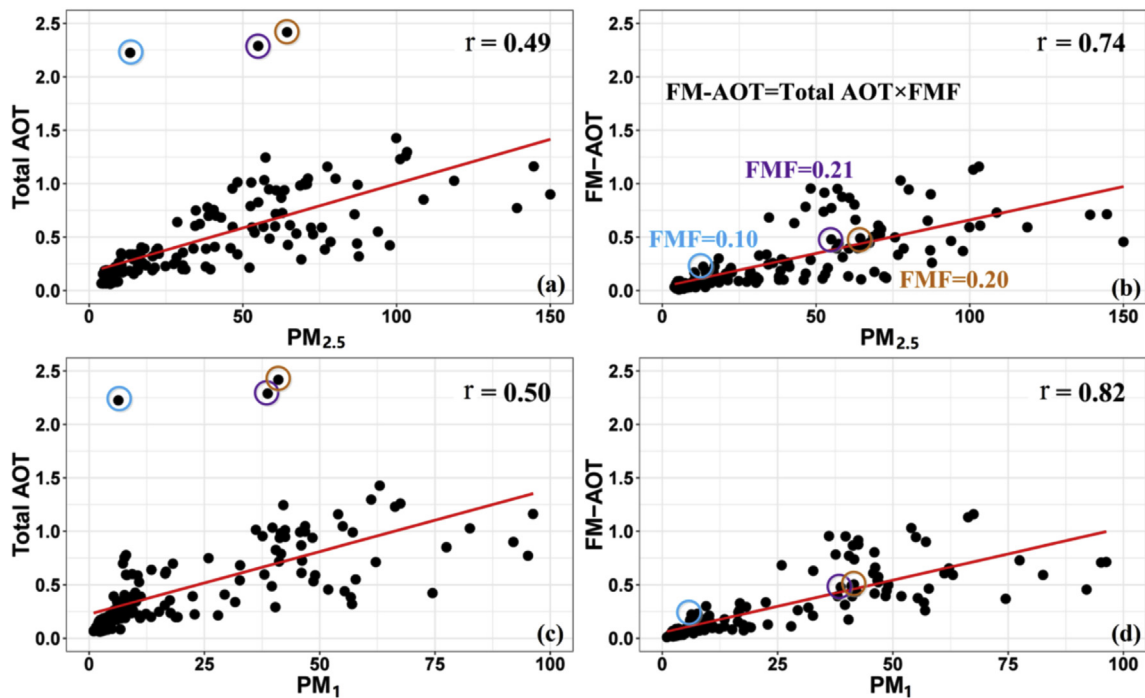

Fig. 6. Comparison between hourly total AOT- and FM-AOT-based PM$_{2.5}$ and PM$_1$ estimation (N = 146). The red line is the fitted line. The three colored circles show a low FMF but a high total AOT. Comparisons (a) between total AOT and PM$_{2.5}$, (b) between FM-AOT and PM$_{2.5}$, (c) between total AOT and PM$_1$, and (d) between FM-AOT and PM$_1$ are described. (For interpretation of the references to colour in this figure legend, the reader is referred to the web version of this article.)

calculated from AERONET and MODIS FMF are presented in Fig. 7. It can be seen that the LUT-SDA FMF values are in close agreement with the AERONET FMF values. The mean absolute errors (MAE) between LUT-SDA FMF and AERONET FMF at the three selected stations were 0.146 (RADI), 0.149 (Beijing), and 0.159 (CAMS). However, MODIS FMF data were missing for most of the study period. Levy et al. (2010) considered MODIS-retrieved FMF over

land to still be an experimental product with little physical validity. Li et al. (2016) also mentioned limitations relating to the accuracy of MODIS retrieval parameters with respect to the application and validation of Eq. (1). Although there are still limitations for satellite retrieval FMF, as reported in Yan et al. (2017), it provides a spatial view of FMF for each pixel of the satellite image, whereas field measurements only provide point scale outcomes.
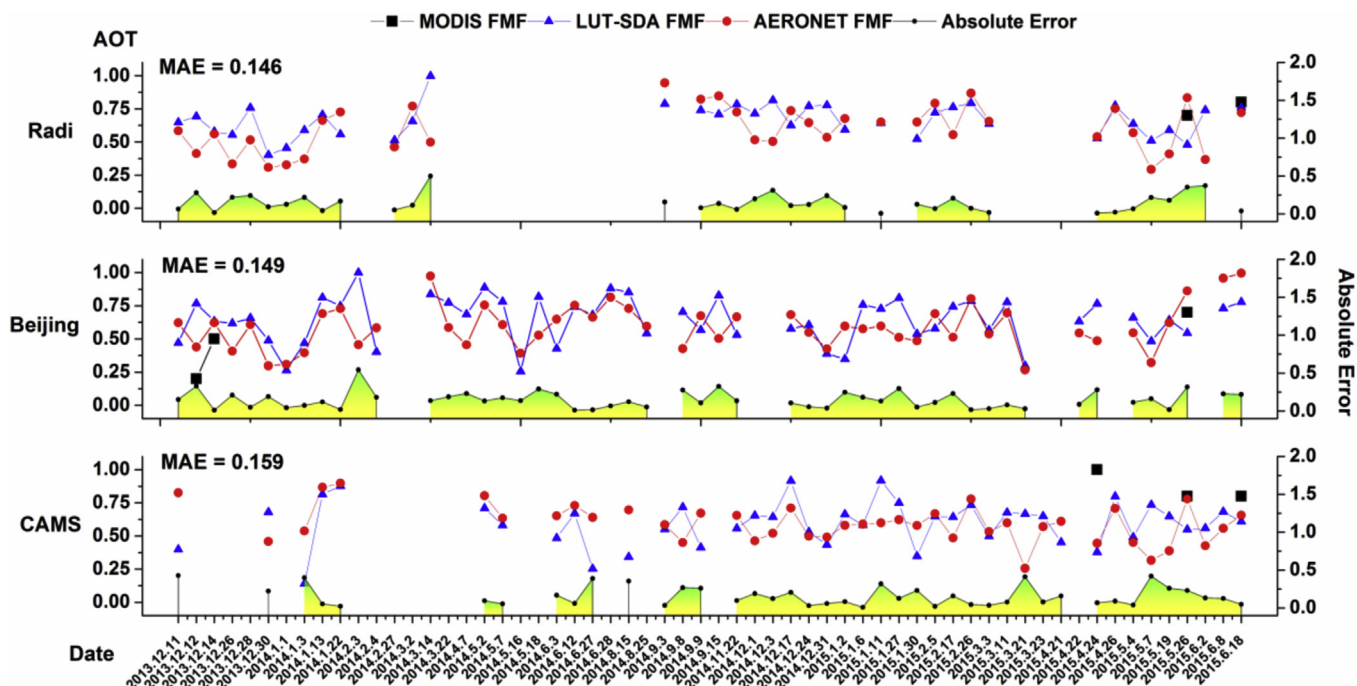
Fig. 7. Comparisons among AERONET FMF, MODIS C6 FMF, and LUT-SDA FMF for different AERONET stations. The MAE is the mean absolute error. The green and yellow shadings show the absolute error between LUT-SDA FMF and AERONET FMF. (For interpretation of the references to colour in this figure legend, the reader is referred to the web version of this article.)

4.2. Pseudo-density for PM2.5

Several studies have reported strong seasonal and diurnal variations in the particle density of $PM_{2.5}$ (Zhao et al., 2013; Wang et al., 2014; Liu et al., 2015). As shown in Table 3, the density of $PM_{2.5}$ in the warm season is always higher than that in the cold season. On average, the density of $PM_{2.5}$ in Beijing can increase from 1.68 g/cm^3 in the cold season to 1.81 g/m^3 in the warm season, due to the contribution from organic matter during the cold season (Liu et al., 2015). Thus, it is problematic to use a constant empirical $PM_{2.5}$ density value in Beijing and it is necessary to use an estimate of ambient particle density for $PM_{2.5}$ to improve the accuracy of surface $PM_{2.5}$ retrieval. Therefore, in this study, we proposed a pseudo-density to address this issue. Based on Chen et al. (2010), $PM_{2.5}$ can be directly calculated from the VIS through the power functions under different RH conditions, as shown in Table 2. And then using Eqs. (4) and (5), we calculated the daily pseudo-density of $PM_{2.5}$ during the study period. As shown in Fig. 8, the pseudo-density of $PM_{2.5}$ showed significant diurnal variations due to changes in weather and pollution conditions. The maximum daily $PM_{2.5}$ pseudo-density could be greater than 2.5 g/cm^3, and the minimum could be less than 0.5 g/cm^3. The results from statistical

Table 3
Density of $PM_{2.5}$ in Beijing from the literature.

Reference	Density (g/cm³)	Sampling time
Liu et al. (2015)	1.60±0.43	July to September 2014
	1.41±0.40	November 2013 to January 2014
Zhao et al. (2013)	1.66±0.74	January to February 2010
	1.82±0.33	July to August 2009
Gao et al. (2007)	1.5	April to August 2005
Cao et al. (2012)	1.79±0.23	June to July 2003
	1.65±0.37	January 2003
Wang et al. (2014)	1.72±0.94	December 2002 to February 2003
	1.82±0.47	July to August 2002

analyses of $PM_{2.5}$ pseudo-density are shown in Fig. 9. The mean value was 1.02 g/cm^3, with a confidence interval of 0.97−1.06 g/cm^3, and the maximum standard deviation was 0.62. Figs. 8 and 9 show that assuming daily variability in $PM_{2.5}$ density in the retrieval model is more appropriate than assuming constant density.

4.3. PM2.5 retrieval results and validation

To illustrate the outcomes of the $PM_{2.5}$ retrieval model proposed in this study, we used two retrieval results as examples. Fig. 10 shows estimated $PM_{2.5}$ concentrations on 6 January 2015. It can be seen that the AOT retrieved using the SARA ranged from 0.05 to 0.27, and its highest values were always centered in the south of Beijing (Fig. 10A). The FMF derived from the LUT-SDA presented high values in central and south-eastern urban areas that have continually high traffic flow and dense populations (Fig. 10B). These areas with high FMF indicate a significant contribution of fine particles to the total AOT. The PBLH and RH produced by the WRF are shown in Fig. 10 C and E. There is a marked difference in the spatial coverage of PBLH on this day (There is also a significant difference in the spatial distribution of PBLH in other study days, as shown in Figs. S1−S4). In the north of Beijing, PBLH reached 605−746 m, and in most central areas was more than 474 m, whereas in the east and west of Beijing, PBLH was 366−417 m. Fig. 10E shows that the RH decreased gradually from the north-west (0.29−0.33) to the south-east (0.18−0.21) of Beijing. The f (RH) corresponding to RH is shown in Fig. 10D. It can be seen that its spatial pattern is similar to that in Fig. 10E. Finally, the derived $PM_{2.5}$ is presented in Fig. 10F. The spatial distribution pattern of $PM_{2.5}$ spatial distribution pattern is similar to that of AOT shown in Fig. 10A. High levels of $PM_{2.5}$ in southern and eastern urban areas are clearly visible, indicating that anthropogenic pollution was heavy in these areas. However, the $PM_{2.5}$ mass concentration was low (6−23 μg/m^3) in northern rural areas.
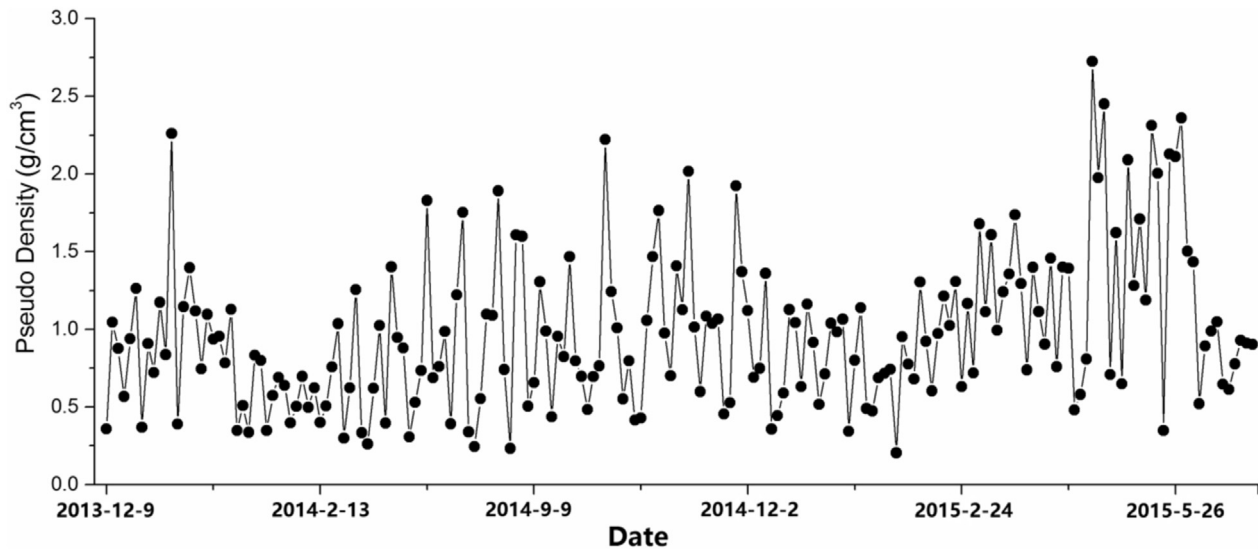
Fig. 8. Variation in PM$_{2.5}$ pseudo-density (g/cm^3) from December 2013 to June 2015.
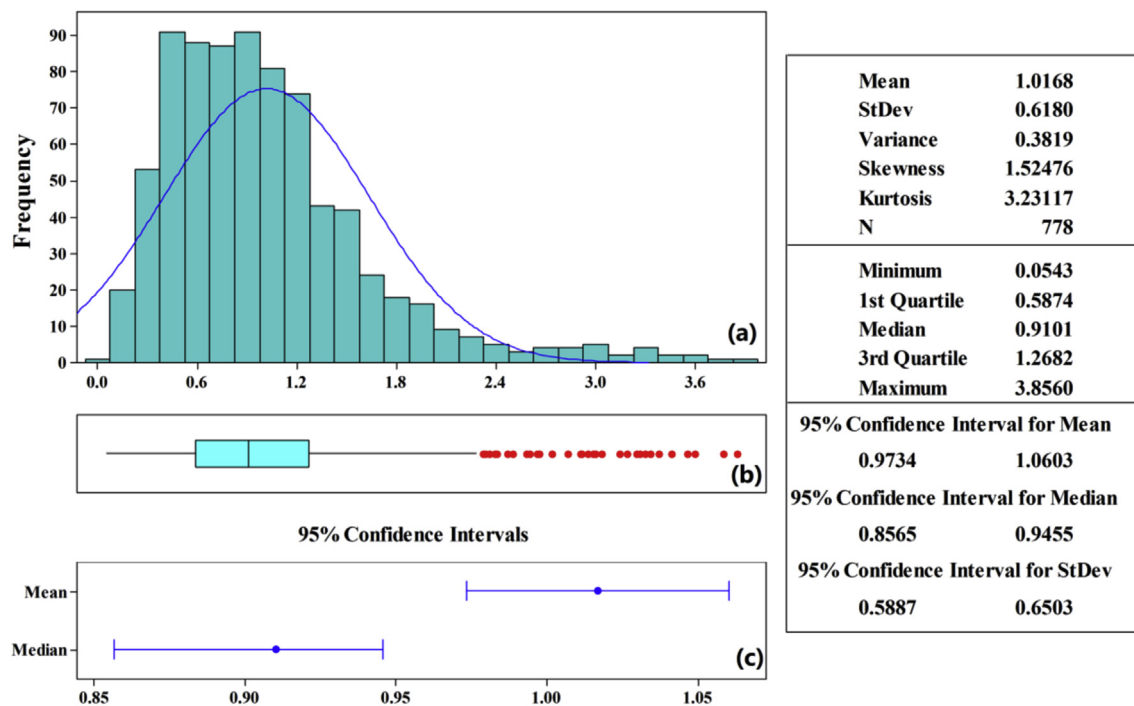

Fig. 9. Statistical analyses of PM$_{2.5}$ pseudo-density (g/cm^3) during the study period. Figure (a) is the histogram of PM$_{2.5}$ pseudo-density, (b) is the boxplot of PM$_{2.5}$ pseudo-density, and (c) is the interval plot for mean and median of PM$_{2.5}$ pseudo-density.

To test the performance of the PM$_{2.5}$ retrieval model developed in this study, we extended the PM$_{2.5}$ retrieval to the areas surrounding Beijing. The test data were obtained on 16 October 2014 and the derived results are shown in Fig. 11. High AOT was observed in the south of Beijing, east of Tianjin, and south-west and east of Hebei (Fig. 11A). From Fig. 11B, it can be seen that FMF values were high in the center of Beijing, south of Hebei and east of Tianjin. The PM$_{2.5}$ retrieval results are shown in Fig. 11C. It can be seen that high-PM$_{2.5}$ polluted regions occurred in the south of Beijing and Hebei, and also in the east of Tianjin. These results are consistent with Zhang and Li (2015), Ma et al. (2014), and Zheng et al. (2016). Comparing Fig. 11 A and C, the derived PM$_{2.5}$ has a similar spatial

pattern to AOT, but with some differences due to the incorporation of FMF, RH, and PBLH corrections, such as in the area of Beijing where the AOT was low, but the PM$_{2.5}$ concentration was high.

Fig. 12A shows the mean PM$_{2.5}$ concentration from satellite-retrieved data and ground-based measurements from December 2013 to June 2015. High PM$_{2.5}$ levels can be seen clearly in the southern urban region. PM$_{2.5}$ concentrations in these areas were 42–44 μg/m^3 from satellite retrieval, and 42–48 μg/m^3 from ground-based measurements. In contrast, PM$_{2.5}$ levels were significantly lower in the rural areas north and west of Beijing, where the population is sparse and there are fewer vehicles. Fig. 12A shows that there is close agreement between the satellite-
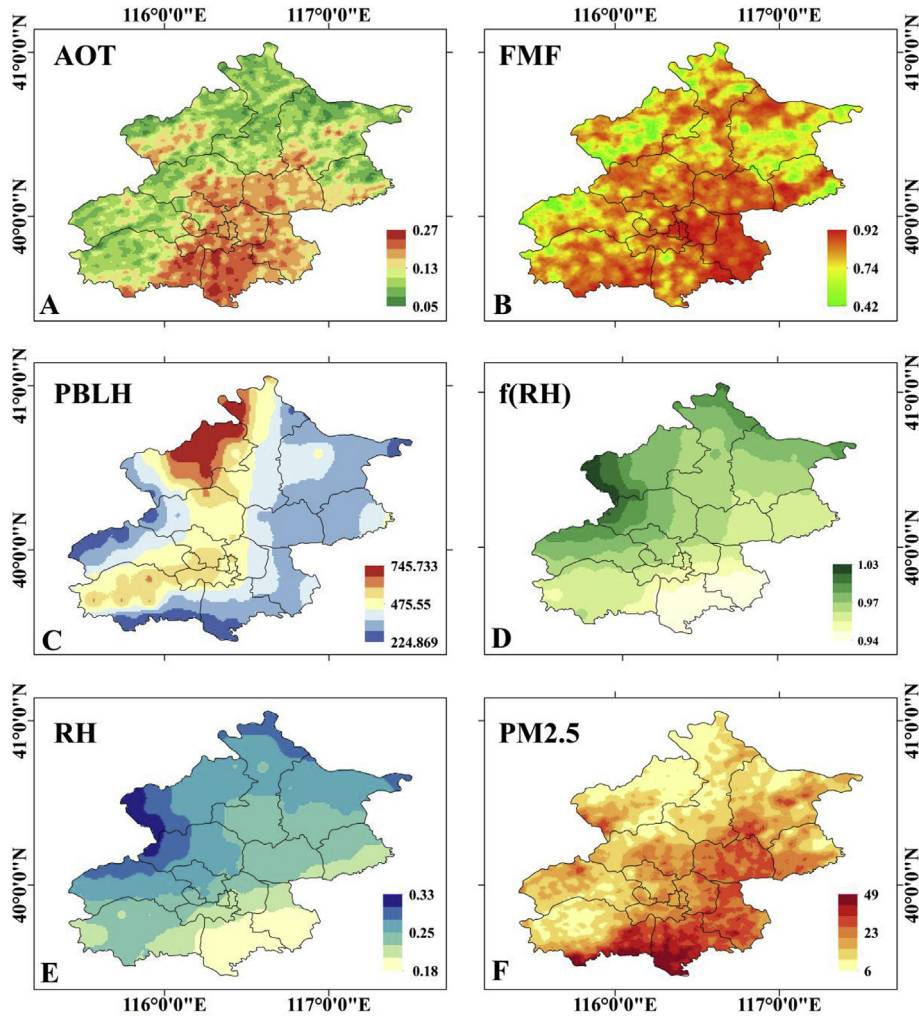
Fig. 10. Estimation of PM$_{2.5}$ on 6 January 2015. A is the AOT retrieved from SARA, B is the FMF result calculated by LUT-SDA, C is the PBLH (units: m), D is the optical hydroscopic growth function by Eq. (3), E is the RH, and F is the estimated PM$_{2.5}$ by Eq. (1) (units: μg/m^3).
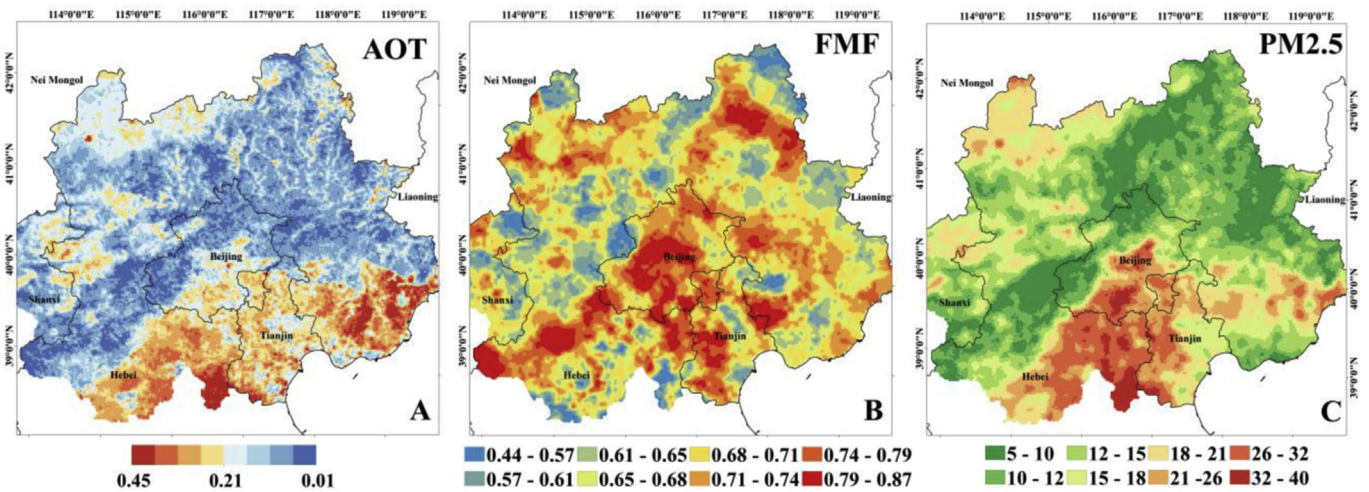

Fig. 11. Extension of PM$_{2.5}$ retrieval to the Beijing neighborhood. A is the AOT retrieved from SARA, B is the FMF by LUT-SDA, and C is the estimated PM$_{2.5}$ by Eq. (1) (units: μg/m^3).

retrieved data and *in situ* measurements, and the derived PM$_{2.5}$ spatial distribution was similar to that reported by Li et al. (2015).

Fig. 12B presents the validation results of derived PM$_{2.5}$ with 921 *in situ* PM$_{2.5}$ measurements. Linear regression gave a slope of 0.67 and
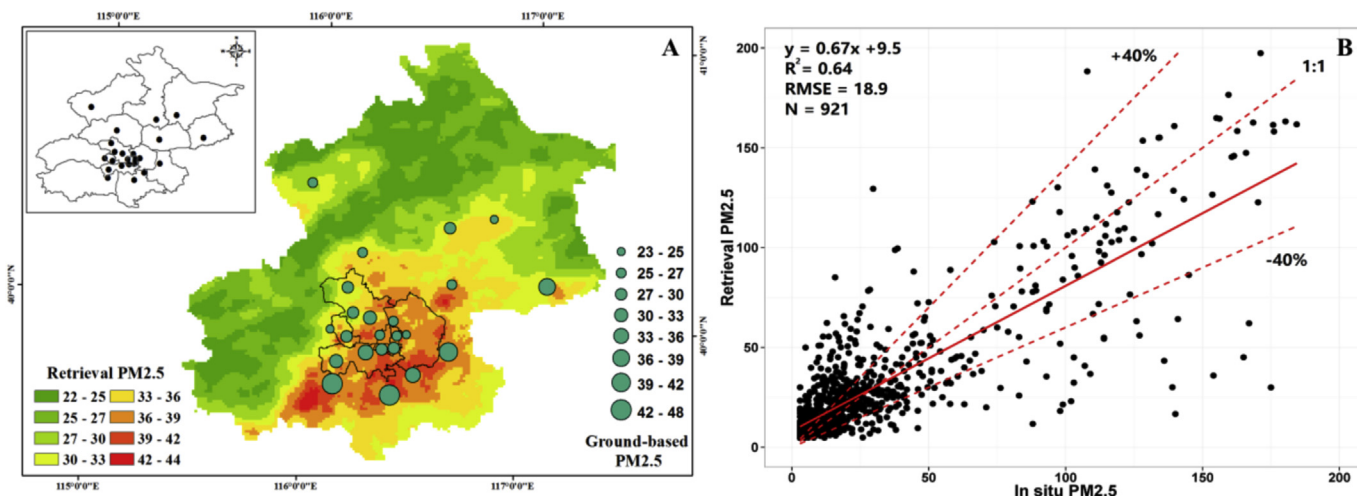
Fig. 12. Mean PM$_{2.5}$ from December 2013 to June 2015. (A), and validation (B). Units: μg/m^3. Dotted red lines show the estimated error envelope line $\pm 0.4 \cdot PM2.5_{in\ situ}$, and the solid red line shows the 1:1 line. (For interpretation of the references to colour in this figure legend, the reader is referred to the web version of this article.)

an intercept of 9.5, with a coefficient of determination (R^2) of 0.67 (N = 921) and RMSE of 18.9 μg/m^3. The validation results showed that the derived PM$_{2.5}$ agreed closely with *in situ* observations, indicating that the retrieval model performed well.

5. Discussion

In this study, we found that FM-AOT was more closely correlated than total AOT with ground-level PM$_{2.5}$ concentration. In contrast, Wang et al. (2015a) reported a significantly lower correlation when total AOT was replaced by FM-AOT for PM$_{2.5}$ estimation. This inconsistency may be because the PM$_{2.5}$ and AOT data were not collected from the same locations: the straight-line distance between the sites where the data on the two variables were collected was about 3000 m in Wang et al. (2015a). However, in this study, the PM$_{2.5}$ and AOT data were collected from the exact same location. For the comparisons of FMF between MODIS, LUT-SDA and AERONET, we observed that the MODIS FMF data had significant uncertainties and large amounts of data were unavailable. Because of this issue, the MAE of the PM$_{2.5}$ retrieval results in Zhang and Li (2015) was 64 μg/m^3 using MODIS FMF, which is quite large. One possible reason for this is that the relationship between VE$_f$ and FMF is based on the inversion method AERONET data in Eq (2); however, the FMF from the MODIS C6 product is derived using a different method and has a different definition. There can be highly significant uncertainties in the VE$_f$ calculation using the MODIS C6 FMF relative to the AERONET FMF. Therefore, this can be a significant limitation for the application of Eqs. (1) and (2). To address this problem, we used the LUT-SDA FMF in this study, which is more reliable, as shown in Fig. 7. In addition, assuming a constant density is inappropriate for real-time PM$_{2.5}$ estimation due to distinct diurnal and seasonal variations (Liu et al., 2015). Hoff and Christopher (2009) suggested that satellite AOT should be combined with ground-based measurements to improve PM estimation from space. Therefore, using VIS data from weather stations, the intraday pseudo-density was calculated for each satellite image. Although this provides only rough density estimation, it is important for real-time surface PM$_{2.5}$ retrieval and produces an accurate PM$_{2.5}$ with a RMSE of 18.9 μg/m^3.

6. Conclusion

Based on ground-based measurements obtained in Xingtai city,

China during May–June 2016, surface Particulate Matter$_{2.5}$ (PM$_{2.5}$) was found to have a closer correlation with the Fine Mode-Aerosol Optical Thickness (FM-AOT) (r = 0.74) than with the total AOT (r = 0.49). We established a PM$_{2.5}$ retrieval model incorporating look-up table−spectral deconvolution algorithm (LUT-SDA) fine mode fraction (FMF) (Yan et al., 2017), SARA AOT (Bilal et al., 2013), and the PM$_{2.5}$ remote sensing method (Zhang and Li, 2015). Compared with Aerosol Robotic Network (AERONET) data, the LUT-SDA FMF was found to be more reliable than the MODIS FMF. The mean absolute errors (MAEs) between AERONET FMF and LUT-SDA FMF were 0.146 in RADI, 0.149 in Beijing, and 0.159 in CAMS. Due to significant diurnal variation in the density of PM$_{2.5}$, we proposed a pseudo-density to enhance PM$_{2.5}$ estimation based on real-time visibility (VIS) data. The standard deviation of the PM$_{2.5}$ pseudo-density was 0.62, which also varied diurnally due to changing weather and pollution conditions; this finding is consistent with previous studies (Zhao et al., 2013; Wang et al., 2014; Liu et al., 2015). The performance of the ground-level PM$_{2.5}$ retrieval model developed in this study was tested over Beijing from December 2013 to June 2015. The retrieval results compared to 30 *in situ* sites showed that the model performed well (R^2 = 0.64, root mean square error (RMSE) = 18.9 μg/m^3 [N = 921]). Furthermore, the retrieval results demonstrated that the developed model was able to monitor air pollutants in the Beijing regions with full spatial coverage and temporal resolution.

Appendix A. Supplementary data

Supplementary data related to this article can be found at https://doi.org/10.1016/j.atmosenv.2017.09.023.

References

Anderson, J.O., Thundiyil, J.G., Stolbach, A., 2012. Clearing the air: a review of the effects of particulate matter air pollution on human health. J. Med. Toxicol. 8, 166–175.

Bai, Y., Qi, H., Liu, L., Chen, C., Lin, C., Li, W., 2016. Study on the nonlinear relationship among the visibility, PM2.5 concentration and relative humidity in Wuhan and the visibility prediction. Acta Meteorol. Sin. 74, 189–199.

Bell, M., Ebisu, K., Peng, R., 2011. Community-level spatial heterogeneity of chemical levels of fine particulates and implications for epidemiological research. J. Expo. Sci. Env. Epid. 21, 372–384.

Bilal, M., Nichol, J.E., Bleiweiss, M.P., Dubois, D., 2013. A Simplified high resolution MODIS Aerosol Retrieval Algorithm (SARA) for use over mixed surfaces. Remote Sens. Environ. 136, 135–145.

Bilal, M., Nichol, J.E., Chan, P.W., 2014. Validation and accuracy assessment of a Simplified Aerosol Retrieval Algorithm (SARA) over Beijing under low and high aerosol loadings and dust storms. Remote Sens. Environ. 153, 50–60.

Brook, R.D., Rajagopalan, S., Pope, C.A., Brook, J.R., Bhatnagar, A., Diez-Roux, A.V., Holguin, F., Hong, Y., Luepker, R.V., Mittleman, M.A., Peters, A., Siscovick, D., Smith Jr., S.C., Whitsel, L., Kaufman, J.D., American Heart Association Council on Epidemiology and Prevention, Council on the Kidney in Cardiovascular Disease, Council on Nutrition, Physical Activity and Metabolism, 2010. Particulate matter air pollution and cardiovascular disease: an update to the scientific statement from the American Heart Association. Circulation 121, 2331–2378.

Cao, J.J., Shen, Z.X., Chow, J.C., Watson, J.G., Lee, S.C., Tie, X.X., Ho, K.F., Wang, G.H., Han, Y.M., 2012. Winter and summer PM2.5 chemical compositions in fourteen Chinese cities. J. Air Waste Manag. Assoc. 62, 1214–1226.

Chen, D., Liu, X., Lang, J., Zhou, Y., Wei, L., Wang, X., Guo, X., 2017. Estimating the contribution of regional transport to PM$_{2.5}$ air pollution in a rural area on the North China Plain. Sci. Total Environ. 583, 280–291.

Chen, Y.Z., Zhao, D., Chai, F.H., Liang, G.X., Xue, Z.G., Wang, B.B., Liang, Y.J., Chen, Y., Zhang, M., 2010. Correlation between the atmospheric visibility and aerosol fine particle concentrations in guangzhou and beijing. China Environ. Sci. 30, 967–971.

Chen, Y., Zhao, P., He, D., Dong, F., Zhao, X., Zhang, X., 2015. Character and parameterization for atmospheric coefficient in Beijing. Environ. Sci. 36, 3582–3589. https://doi.org/10.13227/j.hjkx.2015.10.005.

Cheng, M., Zhi, G., Tang, W., Liu, S., Dang, H., Guo, Z., et al., 2017. Air pollutant emission from the underestimated households' coal consumption source in China. Sci. Total Environ. 580, 641–650.

Chudnovsky, A., Kostinski, A., Lyapustin, A., Koutrakis, P., 2013. Spatial scales of pollution from variable resolution satellite imaging. Environ. Pollut. 172, 131–138.

Chudnovsky, A.A., Koutrakis, P., Kloog, I., Melly, S., Nordio, F., Lyapustin, A., et al., 2014. Fine particulate matter predictions using high resolution aerosol optical depth (AOD) retrievals. Atmos. Environ. 89, 189–198.

Dawson, J.P., Adams, P.J., Pandis, S.N., 2007. Sensitivity of PM 2.5 to climate in the Eastern US: a modeling case study. Atmos. Chem. Phys. 7 (16), 4295–4309.

Eeftens, M., Beelen, R., de Hoogh, K., Bellander, T., Cesaroni, G., Cirach, M., et al., 2012. Development of land use regression models for PM2.5, PM2.5 absorbance, PM10 and PMcoarse in 20 European study areas; results of the ESCAPE project. Environ. Sci. Technol. 46, 11195–11205.

Elminir, H.K., 2005. Dependence of urban air pollutants on meteorology. Sci. Total Environ. 350 (1), 225–237.

Engel-Cox, J.A., Holloman, C.H., Coutant, B.W., Hoff, R.M., 2004. Qualitative and quantitative evaluation of MODIS satellite sensor data for regional and urban scale air quality. Atmos. Environ. 38, 2495–2509.

Gao, J., Zhou, Y., Wang, J., Wang, W., 2007. Inter-comparison of WPS™-TEOM™-MOUDI™ and investigation on particle density. Environ. Sci. 28, 1929–1934.

Gasso, S., O'Neill, N., 2006. Comparison of remote sensing retrievals and in situ measurements of aerosol fine mode fraction during ACE-Asia. Geophys. Res. Lett. 33, L05807.

Grguric, S., Krizan, J., Gasparac, G., Oleg, A., et al., 2014. Relationship between MODIS based aerosol optical depth and PM10 over Croatia. Cent. Eur. J. Geosci. 6, 2–16.

Guo, Y.J., Feng, N., Christopher, S.A., Kang, P., Zhan, F.B., Hong, S., 2014. Satellite remote sensing of fine particulate matter (PM2.5) air quality over Beijing using MODIS. Int. J. Remote Sens. 35, 6522–6544.

Gupta, P., Christopher, S.A., Wang, J., Gehrig, R., Lee, Y., Kumar, N., 2006. Satellite remote sensing of particulate matter and air quality assessment over global cities. Atmos. Environ. 40, 5880–5892.

Gupta, P., Christopher, S.A., 2009. Particulate matter air quality assessment using integrated surface, satellite, and meteorological products: multiple regression approach. J. Geophys. Res. – Atmos. 114, D14205.

Han, Y., Wu, Y., Wang, T., Zhuang, B., Li, S., Zhao, K., 2015. Impacts of elevated-aerosol-layer and aerosol type on the correlation of AOD and particulate matter with ground-based and satellite measurements in Nanjing, southeast China. Sci. Total Environ. 532, 195–207.

Hoff, R.M., Christopher, S.A., 2009. Remote sensing of particulate pollution from space: have we reached the promised land? J. Air & Waste Manag. Assoc. 59, 645–675.

Holben, B.N., Eck, T.F., Slutsker, I., Tanré, D., Buis, J.P., Setzer, A., Vermote, E., Reagan, J.A., Kaufman, Y., Nakajima, T., Lavenu, F., Jankowiak, I., Smirnov, A., 1998. AERONET - a federated instrument network and data archive for aerosol characterization. Rem. Sens. Environ. 66, 1–16.

Holben, B.N., Tanré, D., Smirnov, A., Eck, T.F., Slutsker, I., Abuhassan, N., Newcomb, W.W., Schafer, J.S., Chatenet, B., Lavenu, F., Kaufman, Y.J., Castle, J.V., Setzer, A., Markham, B., Clark, D., Frouin, R., Halthore, R., Karneli, A., O'Neill, N.T., Pietras, C., Pinker, R.T., Voss, K., Zibordi, G., 2001. An emerging ground-based aerosol climatology: aerosol optical depth from AERONET. J. Geophys. Res. 106, 12,067–12,097.

Jerrett, M., Arain, A., Kanaroglou, P., Beckerman, B., Potoglou, D., Sahsuvaroglu, T., et al., 2005. A review and evaluation of intraurban air pollution exposure models. J. Expo. Sci. Environ. Epidemiol. 15, 185–204.

Kim, S.W., Yoon, S.C., Kim, J., Kim, S.Y., 2007. Seasonal and monthly variations of columnar aerosol optical properties over east Asia determined from multi-year MODIS, LIDAR, and AERONET Sun/sky radiometer measurements. Atmos. Environ. 41 (8), 1634–1651.

Kloog, I., Ridgway, B., Koutrakis, P., Coull, B.A., Schwartz, J.D., 2013. Long- and short-term exposure to PM2.5 and mortality. Epidemiology 24, 555–561.

Kloog, I., Sorek-Hamer, M., Lyapustin, A., Coull, B., Wang, Y., C.Just, A., Schwartz, J., M.Broday, D., 2015. Estimating daily PM2.5 and PM10 across the complex geo-climate region of Israel using MAIAC satellite-based AOD data. Atmos. Environ. 122, 409–416.

Kokhanovsky, A.A., Prikhach, A.S., Katsev, I.L., Zege, E.P., 2009. Determination of particulate matter vertical columns using satellite observations. Atmos. Meas. Tech. 2, 327–335.

Lee, H.J., Coull, B.A., Bell, M.L., Koutrakis, P., 2012. Use of satellite-based aerosol optical depth and spatial clustering to predict ambient PM2.5 concentrations. Environ. Res. 118, 8–15.

Lee, H.J., Liu, Y., Coull, B.A., Schwartz, J., Koutrakis, P., 2011. A novel calibration approach of MODIS AOD data to predict PM2.5 concentrations. Atmos. Chem. Phys. 11, 7991–8002.

Leung, Y., Wu, M., Yeung, K., 2008. A study on the relationship among visibility, atmospheric suspended particulate concentration and meteorological conditions in Hong Kong. Acta Meteorol. Sin. 66, 461–469.

Levy, R., Remer, L., Mattoo, S., Vermote, E., Kaufman, Y.J., 2007. Second-generation operational algorithm: retrieval of aerosol properties over land from inversion of Moderate Resolution Imaging Spectroradiometer spectral reflectance. J. Geophys. Res.-Atmos. 112, D13211.

Levy, R.C., Remer, L.A., Kleidman, R.G., Mattoo, S., Ichoku, C., Kahn, R., Eck, T.F., 2010. Global evaluation of the Collection 5 MODIS dark-target aerosol products over land. Atmos. Chem. Phys. 10, 10399–10420.

Li, R., Gong, J., Chen, L., Wang, Z., 2015. Estimating ground-level PM2.5 using fine-resolution satellite data in the megacity of Beijing, China. Aerosol Air Qual. Res. 15, 1347–1356.

Li, Z., Zhang, Y., Shao, J., et al., 2016. Remote sensing of atmospheric particulate mass of dry PM2.5 near the ground: method validation using ground-based measurements. Remote Sens. Environ. 173, 59–68.

Liu, Y.J., Zhang, T.T., Liu, Q.Y., Zhang, R.J., Sun, Z.Q., Zhang, M.G., 2014. Seasonal variation of physical and chemical properties in TSP, PM10 and PM2. 5 at a roadside site in Beijing and their influence on atmospheric visibility. Aerosol Air Qual. Res. 14 (3), 954–969.

Liu, Y., Paciorek, C.J., Koutrakis, P., 2009. Estimating regional spatial and temporal variability of PM2.5 concentrations using satellite data, meteorology, and land use information. Environ. Health Perspect. 117, 886–892.

Liu, Y., Wang, Z., Wang, J., Welton, E.J., Ferrare, R.A., Newson, R.K., 2011. The effect of aerosol vertical profiles on satellite-estimated surface particle sulfate concentrations. Remote Sens. Environ. 508–513.

Liu, Z., Hu, B., Ji, D., Wang, Y., Wang, M., Wang, Y., 2015. Diurnal and seasonal variation of PM2.5 apparent particle density in Beijing, China. Atmos. Environ. 120, 328–338.

Luo, N., Wong, M.S., Zhao, W., Yan, X., Xiao, F., 2015. Improved aerosol retrieval algorithm using Landsat images and its application for PM10 monitoring over urban areas. Atmos. Res. 153, 264275.

Luo, N., Zhao, W., Yan, X., 2014. Integrated aerosol optical thickness, gaseous pollutants and meteorological parameters to estimate ground PM2.5 concentration. Fresenius Environ. Bull. 23, 2567–2577.

Ma, Z., Hu, X., Huang, L., Bi, J., Liu, Y., 2014. Estimating ground-level PM2.5 in China using satellite remote sensing. Environ. Sci. Technol. 48, 7436–7444.

Munchak, L.A., Levy, R.C., Mattoo, S., Remer, L.A., Holben, B.N., Schafer, J.S., Hostetler, C.A., Ferrare, R.A., 2013. MODIS 3 km aerosol product: applications over land in an urban/suburban region. Atmos. Meas. Tech. 6, 1747–1759.

Nicolantonio, W.D., Cacciari, A., Bolzacchini, E., Ferrero, L., Volta, M., Pisoni, E., 2007. MODIS aerosol optical properties over north Italy for estimating surface-level PM2.5. In: Proceedings of Envisat Symposium 2007. Montreux, Switzerland, ESA, SP-636.

Paciorek, C.J., Liu, Y., Moreno-Macias, H., Kondragunta, S., 2008. Spatiotemporal associations between GOES aerosol optical depth retrievals and ground-level PM2.5. Environ. Sci. Technol. 42, 5800–5806.

Pope III, C.A., Burnett, R.T., Thun, M.J., Calle, E.E., Krewski, D., Ito, K., Thurston, G.D., 2002. Lung cancer, cardiopulmonary mortality, and long-term exposure to fine particulate air pollution. Jama 287 (9), 1132–1141.

Pope III, C.A., Ezzati, M., Dockery, D.W., 2009. Fine-particulate air pollution and life expectancy in the United States. N. Engl. J. Med. 2009 (360), 376–386.

Qu, W., Wang, J., Zhang, X., Sheng, L., Wang, W., 2016. Opposite seasonality of the aerosol optical depth and the surface particulate matter concentration over the north China Plain. Atmos. Environ. 127, 90–99.

Schaap, M., Apituley, A., Timmermans, R.M.A., Koelemeijer, R.B.A., de Leeuw, G., 2009. Exploring the relation between aerosol optical depth and PM2.5 at

Cabauw, The Netherlands. Atmos. Chem. Phys. 9, 909—925.

Skamarock, W.C., Klemp, J.B., Dudhia, J., Gill, D.O., Barker, D.M., Wang, W., Powers, J.G., 2005. A Description of the Advanced Research WRF Version 2(No. NCAR/TN-468+ STR). National Center For Atmospheric Research Boulder Co Mesoscale and Microscale Meteorology Div.

Toth, T.D., Zhang, J., Campbell, J.R., Hyer, E.J., Reid, J.S., Shi, Y., Westphal, D.L., 2014. Impact of data quality and surface-to-column representativeness on the PM 2.5/ satellite AOD relationship for the contiguous United States. Atmos. Chem. Phys. 14, 6049—6062.

van Donkelaar, A., Martin, R.V., Brauer, M., Kahn, R., Levy, R., Verduzco, C., Villeneuve, P.J., 2010. Global estimates of ambient fine particulate matter concentrations from satellite-based aerosol optical depth: development and application. Environ. Health Perspect. 118 (6), 847.

van Donkelaar, A., Martin, R.V., Levy, R.C., da Silva, A.M., Krzyzanowski, M., Chubarova, N.E., Semutnikova, E., Cohen, A.J., 2011. Satellite-based estimates of ground-level fine particulate matter during extreme events: a case study of the Moscow fires in 2010. Atmos. Environ. 45, 6225—6232.

Wang, J., 2003. Intercomparison between satellite derived aerosol optical thickness and PM2.5 mass: implications for air quality studies. Geophys. Res. Lett. 30, 2095.

Wang, J.C., Zhu, C.J., Zhu, Y., Chen, S.G., 2015. Correlation between remote sensing aerosol parameters and PM2.5 in Beijing. China Environ. Sci. 35, 1947—1956.

Wang, J.L., Zhang, Y.H., Shao, M., Liu, X.L., 2006. The quantitative relationship between visibility and mass concentration of PM2.5 in Beijing. WIT Trans. Ecol. Environ. 86, 595—610.

Wang, J., Xu, X., Spurr, R., Wang, Y., Drury, E., 2010. Improved algorithm for MODIS satellite retrievals of aerosol optical thickness over land in dusty atmosphere: implications for air quality monitoring in China. Remote Sens. Environ. 114, 2575—2583.

Wang, L., Wei, Z., Wei, W., Fu, J.S., Meng, C., Ma, S., 2015. Source apportionment of PM$_{2.5}$ in top polluted cities in Hebei, China using the CMAQ model. Atmos. Environ. 122, 723—736.

Wang, W., Maenhaut, W., Yang, W., Liu, X.D., Bai, Z.P., Zhang, T., Claeys, M., Cachier, H., Dong, S.P., Wang, Y.L., 2014. One-year aerosol characterization study for PM2.5 and PM10 in Beijing. Atmos. Pollut. Res. 5, 554—562.

WMO, 2008. Guide to Meteorological Instruments and Methods of Observation, seventh ed. WMO No.8.

Xu, X., Wang, J., Henze, D.K., et al., 2013. Constraints on aerosol sources using GEOSChem adjoint and MODIS radiances, and evaluation with multi-sensor (OMI, MISR) data. J. Geophys. Res. — Atmos. 118, 6396—6413.

Yan, X., Li, Z., Shi, W., Luo, N., Wu, T., Zhao, W., 2017. An improved algorithm for retrieving the fine-mode fraction of aerosol optical thickness, part 1: algorithm development. Remote Sens. Environ. 192, 87—97.

Yan, X., Shi, W., Luo, N., Zhao, W., 2016. A new method of satellite-based haze aerosol monitoring over the North China Plain and a comparison with MODIS Collection 6 aerosol products. Atmos. Res. 171, 31—40.

Zhang, Y., Li, Z., 2015. Remote sensing of atmospheric fine particulate matter (PM 2.5) mass concentration near the ground from satellite observation. Remote Sens. Environ. 160, 252—262.

Zhang, Y., Li, Z., 2013. Estimation of PM2.5 from fine-mode aerosol optical depth. J. Remote Sens. 17, 929—943.

Zhao, P., Zhang, X., Xu, X., Zhao, X., 2011. Long-term visibility trends and characteristics in the region of Beijing, Tianjin, and Hebei, China. Atmos. Res. 101 (3), 711—718.

Zhao, P.S., Dong, F., He, D., Zhao, X.J., Zhang, X.L., Zhang, W.Z., Yao, Q., Liu, H.Y., 2013. Characteristics of concentrations and chemical compositions for PM2.5 in the region of Beijing, Tianjin, and Hebei, China. Atmos. Chem. Phys. 13, 4631—4664.

Zheng, B., Zhang, Q., Zhang, Y., He, K.B., Wang, K., Zheng, G.J., Duan, F.K., Ma, Y.L., Kimoto, T., 2015. Heterogeneous chemistry: a mechanism missing in current models to explain secondary inorganic aerosol formation during the January 2013 haze episode in North China. Atmos. Chem. Phys. 15 (4), 2031—2049.

Zheng, Y., Zhang, Q., Liu, Y., Geng, G., He, K., 2016. Estimating ground-level PM2.5 concentrations over three megalopolises in China using satellite-derived aerosol optical depth measurements. Atmos. Environ. 124, 232—242.